ISJ 18: 86-97, 2021 ISSN 1824-307X

RESEARCH REPORT

A C-type lectin (*Aj*SJL-1) containing DPN/WVD motifs in *Apostichopus japonicus* recognizes multiple microbes

Q Zhao[1,4,5], H Wang[1,4,5], W Wang[1,4,5], J Li[1,4,5], Y Liu[1,4,5], Z Xue[1,4,5], Z Liu[1,4,5], L Wang[1,3,4,5], L Song[1,2,3,4,5*]

[1]Liaoning Key Laboratory of Marine Animal Immunology, Dalian Ocean University, Dalian 116023, China
[2]Southern Laboratory of Ocean Science and Engineering (Guangdong, Zhuhai), Zhuhai, 519000, China
[3]Laboratory of Marine Fisheries Science and Food Production Process, Qingdao National Laboratory for Marine Science and Technology, Qingdao 266235, China
[4]Liaoning Key Laboratory of Marine Animal Immunology and Disease Control, Dalian Ocean University, Dalian 116023, China
[5]Dalian Key Laboratory of Aquatic Animal Disease Prevention and Control, Dalian Ocean University, Dalian 116023, China

 Accepted May 14, 2021

Abstract

C-type lectins (CTLs) are a superfamily of Ca^{2+} dependent carbohydrate-recognition proteins with diversified functions ranging from embryonic development to immune defense. In the present study, a CTL containing only one CRD domain with new motifs Asp-Pro-Asn (DPN) and Trp-Val-Asp (WVD) in its Ca^{2+} binding site 2 (designated as *Aj*SJL-1) was identified from sea cucumber *Apostichopus japonicus*. The deduced amino acid sequence of *Aj*SJL-1 was homologous to CTLs from other animals with the identities ranging from 19 % to 28.4 %. The mRNA transcripts of *Aj*SJL-1 were detected in all the examined tissues with varied abundance. The expression level of *Aj*SJL-1 mRNA in coelomocyte was up-regulated significantly at 12 h after *Vibrio splendidus* challenge. The recombinant protein of *Aj*SJL-1 (r*Aj*SJL-1) displayed significant binding activity to lipopolysaccharide, peptidoglycan, mannose and D-galactose in a Ca^{2+}-dependent manner. Moreover, r*Aj*SJL-1 exhibited strong binding capability to *V. splendidus* but week to *Staphylococcus aureus*, *Bifidobacterium breve*, *Pichia pastoris* and *Yarrowia lipolytica* in the presence of Ca^{2+}. These results collectively suggested that *Aj*SJL-1 with new DPN/WVD motifs served as a pattern recognition receptor in sea cucumber with the capability to bind broad-spectrum microbes and initiate the immune response against invaders.

Key Words: C-type lectin; *Apostichopus japonicus*; DPN/WVD motifs; binding capability; innate immunity

Introduction

The C-type lectin (CTL) is a superfamily of Ca^{2+} dependent carbohydrate-recognition proteins with carbohydrate recognition domains (CRDs) (Wang *et al.*, 2011). Most C-type lectins contain one CRD, but some have two or more CRDs (East and Isacke, 2002). Studies in invertebrates have implied that the clustering of multiple CRDs in one molecule endow C-type lectin with broader spectrum and higher affinity of binding pathogen-associated molecular patterns (PAMPs) (Wang *et al.*, 2011). For instance, *Cf*Lec-3 from *Chlamys farreri* with three CRDs can bind more PAMPs than *Cf*Lec-1 and *Cf*Lec-2 with single CRD (Zhang *et al.*, 2009). In addition, the key motifs in CRD of CTLs also affect the recognition range of carbohydrates.

In vertebrate CTLs, there are four Ca^{2+}-binding sites in CRD, among which the Ca^{2+}-binding site 2 is known to be involved in the carbohydrate binding (Zelensky and Gready, 2005). In the Ca^{2+}-binding site 2, the first motif is always Glu-Pro-Asn (EPN) or Gln-Pro-Asp (QPD), which displays specific affinity to mannose or galactose, respectively. The second motif is always Trp-Asn-Asp (WND), which can improve the binding affinity and specificity to carbohydrate (Drickamer, 1992; Zelensky and Gready, 2005).

In invertebrate CTLs, there are many novel motifs such as Glu-Pro-Asp (EPD), Gln-Pro-Gly (QPG), Gln-Pro-Ser (QPS), Tyr-Pro-Gly (YPG), Tyr-Pro-Thr (YPT) for the first motif, and Trp-Ile-Asp (WID), Trp-Ser-Asp (WSD), Trp-His-Asp (WHD), Phe-Ser-Asp (FSD) and Leu-Ser-Asp (LSD) for the

Corresponding author:
Linsheng Song
Dalian Ocean University
Dalian 116023, China
E-mail: lshsong@dlou.edu.cn

Table 1 Designations and nucleotide sequences of the primers were used in this study

Primer	Sequence(5'-3')
*Aj*SJL-1-p1	ATGGCTCTGTCTCTGGTCACTG
*Aj*SJL-1-p2	TTCAATACATGGAAGTTTACAAATGA
*Aj*SJL-1-M1	GGATCCATGGCTCTGTCTCTGGTCACTG
*Aj*SJL-1-M2	GAATTCTTCAATACATGGAAGTTTACAAATGA
Cytb-p1	CGTAGTTCAGTTTCTCCTT
Cytb-p2	AAGGGAAAAGGAAGTGAAAG
T7	TAATACGACTCACTATAGGG
T7-terminator	TGCTAGTTATTGCTCAGCGG
M13-47	CGCCAGGGTTTTCCCAGTCACGAC
M13-48	GAGCGGATAACAATTTCACACAGG
RT-SJL-1-p1	TGCTTCAGTCCATTCAACCGA
RT-SJL-1-p2	GGTCATTTCCGCACCAGTTCT

second motif (Wang *et al.*, 2011). The existence of diversified motifs in invertebrate CTLs suggests that there are flexible binding sites to recognize and bind various carbohydrates, which endow them with multiple immune functions (Huang *et al.*, 2015). For example, a CTL with EPD/WFD motifs (*Cf*Lec-2) from scallop *C. farreri* exhibited the PAMP binding activity to LPS, PGN, mannan, and zymosan (Yang *et al.*, 2010). EPD motif containing lectin *Ai*CTL-7 in scallop *Argopecten irradians* was able to bind LPS, PGN, mannan, yeast glucan and poly I:C *in vitro*, and involved in agglutination of fungi and bacteria (Wang *et al.*, 2011). *Fc*Lec3 with EPS motif identified from Chinese white shrimp *Fenneropenaeus chinensis* recognized muramic acid and peptidoglycan, and functioned in the recognition of bacterial and viral pathogens (Wang *et al.*, 2009). *Pt*CLec1 with YPD motif from swimming crab *Portunus trituberculatus* bound many PAMPs, including lipopolysaccharides (LPS), peptidoglycan (PGN) and glucan (GLU), and numerous microorganisms (Su *et al.*, 2020). The information about the CTLs with novel motifs as well as their functions in the immune response of invertebrates is helpful for the comprehensive understanding of the diversity and complexity of CTL family (Wang *et al.*, 2007; Li *et al.*, 2015b).

Sea cucumber *Apostichopus japonicus* is a special group of marine invertebrates, which is commercially important aquaculture species in Asian countries. Recently, the frequently outbreaks of diseases have caused severe economic losses and threatens the healthy development of sea cucumber framing industry. As an invertebrate, sea cucumber lacks adaptive immunity and solely relies on innate immunity to defend against various invaders. CTL plays an important role in recognizing and binding to microorganisms as PRR in invertebrates to initiate immune responses (Drickamer and Taylor, 1993). The knowledge about CTL family members in *A. japonicus* would provide new insights into the immune defense mechanisms of sea cucumber (Wang *et al.*, 2018). In the present study, a previously identified CTL from *A. japonicus* (Ono *et al.*, 2018) was further investigated with the objectives to (1) characterize new motifs in CRD, (2) examine its mRNA expression after *Vibrio splendidus* challenge, and (3) determine its activity to bind various PAMPs and microbes.

Materials and Methods

Sea cucumber and microbes

Sea cucumbers (*Apostichopus japonicus*) approximately 100 ± 25 g in weight were collected from a local commercial farm (Dalian, China) and maintained in aerated seawater at 18 ± 2 °C for 7 days before experiments.

Lipopolysaccharide (LPS from *Escherichia coli* 055:B5, Sigma-Aldrich, USA), D-galactose (Sigma-Aldrich, USA), peptidoglycan (PGN from *Staphylococcus aureus*, Sigma-Aldrich, USA) and mannose (Man from *Saccharomyces cerevisiae*, Sigma-Aldrich, USA) were dissolved in TBS-Ca^{2+} buffer (50 mM Tris-HCl, 50 mM NaCl, 20 mM $CaCl_2$, pH 7.4) or TBS buffer (50 mM Tris-HCl, 50 mM NaCl, pH 7.4) at the final concentration of 1 M, respectively. These solutions were stored at -20 °C for following experiment.

Gram-negative bacteria *Vibrio splendidus* and *Vibrio anguillarum* (laboratory preservation), Gram-positive bacteria *Streptococcus aureus* (laboratory preservation), *Bifidobacterium breve* (Cellbio, Shanghai), and Fungi *Pichia pastoris* and *Yarrowia lipolytica* (laboratory preservation) were cultured in 2216E medium (Solarbio, Beijing) at 28 °C for 24 h, LB medium at 37 °C for 24 h, BS medium (Hopebio, Qingdao) at 37 °C for 24 h, YPD medium (Solarbio, Beijing) at 28 °C for 24 h, respectively.

Tissue collection and immune challenge

Six unstimulated sea cucumbers were sacrificed, and the tissues including body wall, muscle, gonad, gut, tube-foot and respiratory tree were collected to investigate the mRNA distribution of *Aj*SJL-1. Coelomic fluid was also collected and immediately centrifuged at 800 × *g*, 4 °C for 10 min to harvest the coelomocytes. All these tissues and coelomocyte samples were stored at -80 °C after addition of 1 mL Trizol reagent (Thermo Fisher Scientific, China) for subsequent RNA extraction (Ren *et al.*, 2014; Yan *et al.*, 2018).

A total of 72 sea cucumbers were randomly divided into two groups for soaking stimulation. Thirty-six individuals in control group were soaked in 100 L sterile sea water. Another 36 sea cucumbers in the stimulation group were soaked in sterile sea water adding with *V. splendidus* (1×10^9 CFU/mL, dissolved in seawater) (Wang *et al.*, 2018). Then six sea cucumbers were randomly collected from two groups at 0, 3, 6, 12, 24 and 48 h post-challenge (hpc) for coelomocytes collection as previously described (Jiang *et al.*, 2014).

RNA extraction and cDNA synthesis

Total RNA was extracted from the different tissues of sea cucumber *A. japonicus* by using the Easy Pure RNA Kit (TransGen, Beijing, China). The sample was lysed in Trizol reagent and total RNA was extracted in cold chloroform and pelleted by centrifugation. Then the RNA was purified and washed twice in 70 % ethanol for following steps. According to Prime Script™ First Strand cDNA Synthesis Kit (TaKaRa, Dalian, China), the first-strand of cDNA was synthesized at 37 °C for 15 min, and terminated at 85 °C for 5 s. The cDNA mix was stored at 80 °C for subsequent experiments.

Cloning of AjSJL-1 gene

Based on the published sequence (GenBank accession No. LC214944.1), two primers *Aj*SJL-1-p1 and *Aj*SJL-1-p2 (Table 1) were designed to clone the open reading frame (ORF) of *Aj*SJL-1 (Ono *et al.*, 2018). The PCR products were gel-purified, cloned into the pMD19-T simple vector (TransGen, Beijing, China). The recombinant plasmid was transformed into Trans-5α chemically competent cell (TransGen, Beijing, China), and three positive clones were sequenced by Sangon Biotech (Shanghai).

Sequence analysis of AjSJL-1

The sequence of *Aj*SJL-1 was analyzed using the BLAST algorithm at the National Center for Biotechnology Information. The amino acid sequence of *Aj*SJL-1 and its theoretical molecular weight as well as the isoelectric point were predicated with an online translation tool (http://web.expasy.org/translate). The functional domains were revealed by the simple modular architecture research tool (SMART) version 4.0 (http://smart.embl-heidelberg.de/). The presumed tertiary structure of the CRD in *Aj*SJL-1 was established using the SWISS-MODEL prediction algorithm (http://swissmodel.expasy.org/) and displayed by PyMOL according to previous reports (Arnold *et al.*, 2006; Kiefer *et al.*, 2009). Multiple sequences alignment was created by the Clustal X and performed by online tools (http://www.bio-soft.net/sms/). A phylogenetic tree was constructed based on the deduced amino acid sequences of *Aj*SJL-1 and other C-type lectins by the neighbor-joining (NJ) algorithm using the MEGA 4.1 software (Kumar *et al.*, 2004). To derive confidence value for the phylogeny analysis, bootstrap trials were replicated 1000 times.

Quantitative Real-time PCR analysis of AjSJL-1 mRNA expression pattern

The expression patterns of *Aj*SJL-1 in different tissues (coelomocyte, gut, muscle, gonad, tube-foot, body wall, and respiratory tree) were analyzed by using the ABI Quantstudio Sequence Detection System (Applied Biosystems, USA). The fragment of cytochrome b (*cytb*) gene (GenBank accession No. 7802877) amplified with primers Cytb-p1and Cytb-p2 (Table 1) from *A. japonicus* was served as the internal control (Sun *et al.*, 2010). The $2^{-\triangle\triangle Ct}$ method was used to analyze the relative expression levels of *Aj*SJL-1 in different tissues with the calibrator of coelomocyte (Livak and Schmittgen, 2001).

Preparation of recombinant AjSJL-1 and polyclonal antibody

The ORF fragment encoding *Aj*SJL-1 was amplified with specific primers *Aj*SJL-1-M1 and *Aj*SJL-1-M2 (Table 1). The PCR products with *Bam*H I and *Eco*R I sites were cloned into pET-22b expression vector with His-tag (TransGen, Beijing, China). The recombinant plasmid (pET-22b-*Aj*SJL-1) was transformed into Transetta (DE3) chemically competent cell (TransGen, Beijing, China). After PCR screening with T7 primer (Table 1), the positive clones were confirmed by nucleotide sequencing. The positive transformants were incubated in LB medium (containing 50 mg/mL ampicillin) at 37 °C with shaking at 220 rpm. When the culture medium reached OD_{600} of 0.6-0.8, isopropyl β-D-1-thiogalactopyranoside (IPTG, Sigma, USA) was added at the final concentration of 1 mM, and cultured at 16 °C, 100 rpm for additional 12 h. The recombinant protein (designated r*Aj*SJL-1) was purified through the Ni-Sepharose FF column, refolded, verified and quantified, and then stored at -80 °C as previous report (Jiang *et al.*, 2014).

The r*Aj*SJL-1 was used to prepare polyclonal antibody according to the previous report (Wei *et al.*, 2015). Briefly, 500 μL of r*Aj*SJL-1 (0.64 mg/mL) protein was emulsified with 500 μL complete Freund's adjuvant (Sigma, USA) to immunize 6-8 weeks old mice (bought from Dalian Medical University) by subcutaneous implantation. The second and third inoculations were performed on the 14th and 30th day with incomplete Freund's adjuvant (Sigma, USA). The anti-r*Aj*SJL-1 serum was harvested on the 40th day and obliquely placed at 4 °C overnight. The immune serum (containing anti-r*Aj*SJL-1 antibody) was collected after centrifugation at 4 °C, 3000 g for 30min, and stored at -80 °C before use.

The specificity of polyclonal antibody against r*Aj*SJL-1 was verified by western blotting assay. The r*Aj*SJL-1 proteins were subjected to 12% SDS-PAGE, and the proteins in the gel were transferred to a 0.22 μm pore nitrocellulose membrane for western blotting

analysis. The anti-r*Aj*SJL-1 antibody (diluted at 1:1000) was used as the primary antibody, and the HRP-linked goat-anti-mouse IgG (BBI, USA) (diluted at 1:1000) was used as the secondary antibody. The immune-blotted protein bands were visualized by ECL chemiluminescent substrate reagent kit (Thermo Fisher Scientific, China) and developed by Herosbio gel-imaging system (GE Healthcare, USA). Non-immunized mouse serum was used as negative control.

PAMPs binding assay

The PAMPs-binding ability of r*Aj*SJL-1 was examined by enzyme-linked immune sorbent assay (ELISA) according to previous report with some modification (Loizou *et al.*, 1985; Devi *et al.*, 2010; Yang *et al.*, 2016; Liu *et al.*, 2021). Briefly, 100 μL solutions of LPS, PGN, Man and D-galactose dissolved in TBS or TBS-Ca^{2+} buffer at the final concentration of 0.1 mg/mL were used to coat 96-well plate, and the wells were blocked with 3% BSA (Sangon Biotech, China) in TBST (TBS solution containing 0.05 % Tween-20, pH 7.4) at 37 °C for 1 h. After three times of washing with TBST, 100 μL r*Aj*SJL-1 with gradient dilution was added, and the reaction was incubated at 37 °C for 1 h. The same concentration tag protein (rTrx-His) expressed by the pET-32a null vector was added to the wells as negative group at the same time. Meanwhile, the wells filled with 200 μL TBS were used as blank. The plate was firstly incubated with 100 μL of anti-*Aj*SJL-1 serum (1:1000 dilution in 3% BSA) at 37 °C for 1 h, followed by four times of washing with TBST, and then incubated with 100 μL of goat-anti-mouse Ig-alkaline peroxidase conjugate (Sangon Biotech, China) second antibody (1:4000 dilution in 3% BSA). After the last washing, 100 μL of tetramethylbenzidine (TMB) single component substrate solution (Solarbio, Beijing) was added and incubated at 37 °C for 15 min. The reaction was stopped by adding 50 μL of 2 M HCl per well, and the absorbance was measured at 450 nm (TECAN, Switzerland). The light absorption values of r*Aj*SJL-1 group, rTrx-His group and TBS group were employed as sample group (P), negative group (N) and blank group (B), respectively. Samples with P (sample) – B (blank)/N (negative) - B (blank) > 2.1 were considered as positive. Three replications were performed for each sample, and the data were presented as mean ± SD (N = 3).

Microbial binding assay

Microbial-binding activity of r*Aj*SJL-1 was measured according to previous report with some

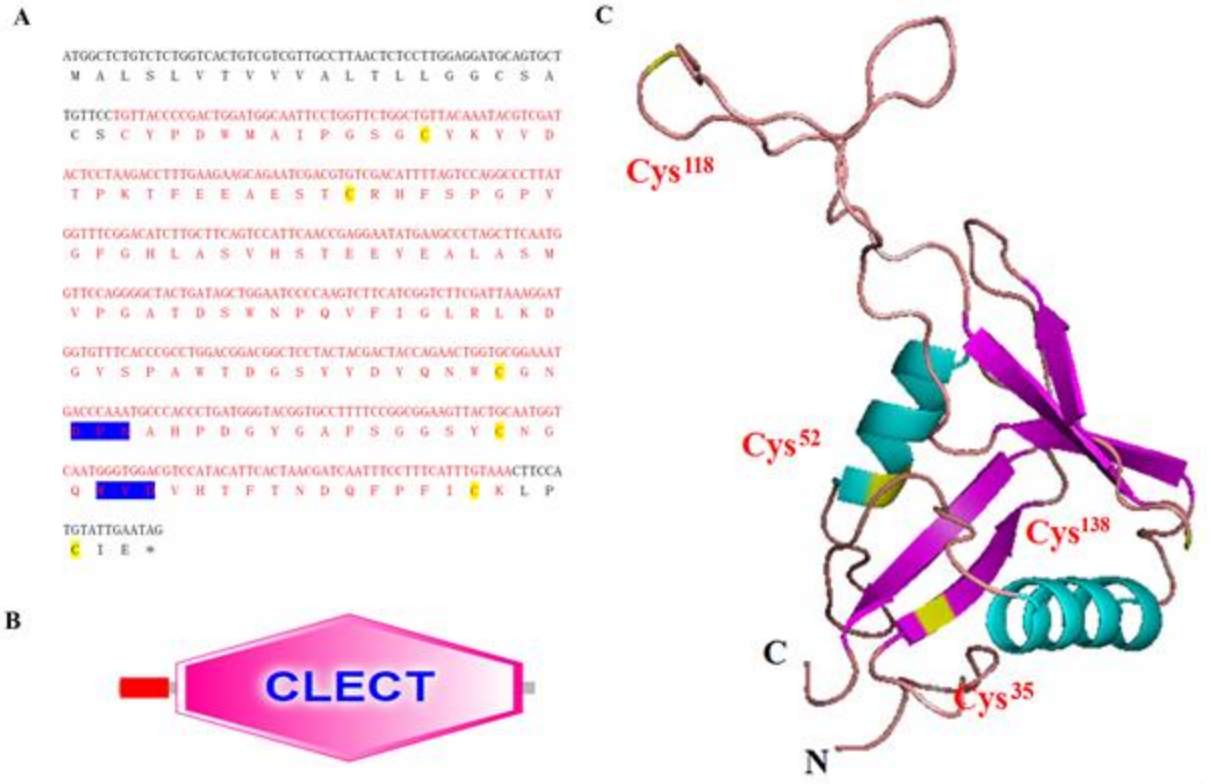

Fig. 1 Sequence features of *Aj*SJL-1. A: Nucleotide and amino acid sequences of *Aj*SJL-1. The motif putative for ligand binding specificity is boxed in blue and the cysteine residues in the CRD are marked with yellow boxes. B: The functional domains predicted by SMART program. Light red represents CRD, and red represents signal peptide. C: The spatial structure of CRD in *Aj*SJL-1 predicted by SWISS-MODEL program. Random coil, β-stands and α-helices are marked as pink, purple, and blue, respectively. There are four cysteines marked as yellow (C^{35}, C^{52}, C^{118}, and C^{138}) involved in forming disulfide bridges

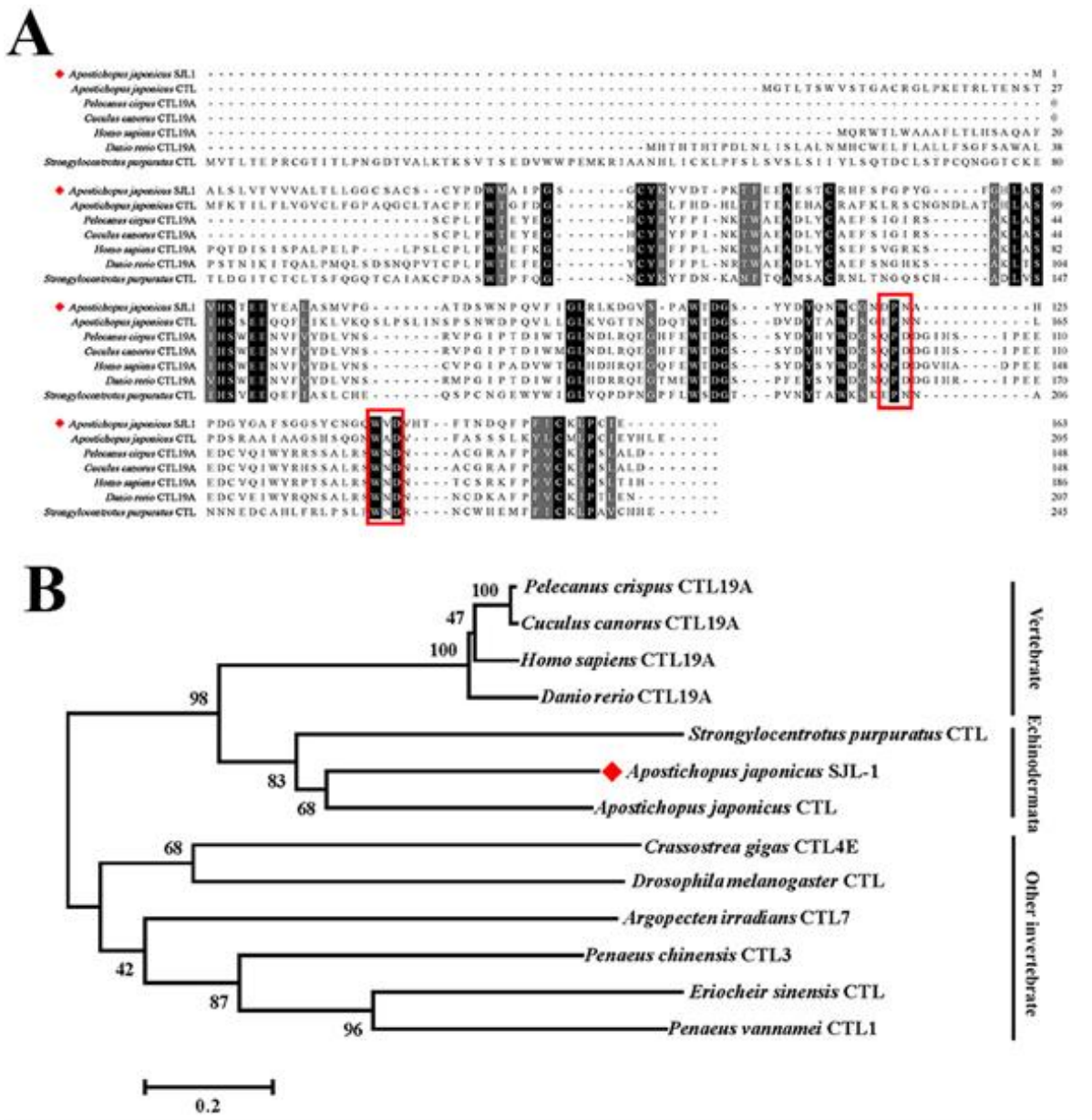

Fig. 2 The multiple sequence alignment and phylogenetic tree of *Aj*SJL-1 with other CTLs. Multiple sequence alignment (A) and Phylogenetic tree (B) of 13 CTL from 12 organisms were analyzed. CTLs from various species include *A. japonicus* (LC214944.1; JN133520), *P. crispus* (KFQ60316.1), *C. canorus* (KFO79987.1), *H. sapiens* (NP_001243649.1), *D. rerio* (NP_001315005.1), *S. purpuratus* (XP_030844747.1), *C. gigas* (EKC23119.1), *Drosophila melanogaster* (ADV37094.1), *Argopecten irradians* (AEE36500.1), *Penaeus chinensis* (ACJ06431.1), *Eriocheir sinensis* (AFF59979.1), *Penaeus vannamei* (ADW08726.1)

modification (Yu *et al.*, 2007). Gram-negative bacteria (*V. splendidus* and *V. anguillarum*), Gram-positive bacteria (*S. aureus* and *B. breve*) and fungi (*P. pastoris* and *Y. lipolytica*) were employed to detect the microbial-binding ability of r*Aj*SJL-1. The microbes were suspended in TBS or TBS-Ca^{2+} buffer, and incubated with r*Aj*SJL-1 (300 μL, 0.64 mg/mL) under slight rotation at 4 °C overnight. After rinsed by TBS for five times, the bound proteins were dissociated from the microorganisms by loading buffer and analyzed by SDS-PAGE and western blot. rTrx (300 μL, 0.5 mg/mL) protein was employed as negative control. The anti-His monoclonal antibody (Sangon Biotech, China) was used for western blot to analysis the bacteria binding activity of rTrx.

Statistical analysis

All data were given as means ± SD and subjected to one-way analysis of variance (one-way ANOVA) followed by a multiple comparison (LSD). Differences were considered significant at $p < 0.05$ (Livak and Schmittgen, 2001).

Results

Molecular characters and predicted spatial structure of AjSJL-1

The ORF sequence of *Aj*SJL-1 was of 492 bp, which encoded a polypeptide of 163 amino acids with molecular mass of 17.74 kDa and theoretical pI of 4.48 (Fig. 1A). There were a signal peptide and only one CRD domain predicted in *Aj*SJL-1 by SMART analysis (Fig. 1B). Two new motifs, DPN and WVD, were identified in CRD domain of *Aj*SJL-1 for carbohydrate binding specificity (Fig. 1A).

The potential tertiary structure of CRD in *Aj*SJL-1 was established by SWISS-MODEL prediction algorithm based on the template 1egi.1.B. The CRD adopted a typical long-form double-loop structure consisting of two parts, a lower part that was constituted of two α-helices and two β-strands, and an upper part that was composed of three β-strands. Moreover, four conserved cysteines (C35, C52, C118, and C138) were predicated to form two disulfide bridges at the bases of the loops. The Cys^{35} and Cys^{138} linked the whole domain loop, while Cys^{52} and Cys^{118} linked the long loop region (Fig. 1C). In addition, another two cysteine residues (Cys^{157} and Cys^{161}) were identified at the N-terminus of the CRD, indicating a long-form CRD in *Aj*SJL-1 (Fig. 1A).

Homology comparison of AjSJL-1

BLAST homology analysis revealed that *Aj*SJL-1 shared 19% to 28.4 % identities with CTLs from *A. japonicus* (JN133520) and other animals, such as *Pelecanus crispus* (KFQ60316.1), *Cuculus canorus* (KFO79987.1), *Homo sapiens* (NP_001243649.1), *Danio rerio* (NP_001315005.1), and *Strongylocentrotus purpuratu*s (XP_030844747.1) (Fig. 2A).

A neighbor-joining tree was constructed based on multiple sequence alignment of *Aj*SJL-1 and other ten CTLs from different species. There were generally three groups in the phylogenetic tree. *Aj*SJL-1 and the CTLs from *A. japonicus* (*Aj*CTL) and *S. purpuratus* (*Sp*CTL) were first clustered into the echinoderm group, which formed a sister group to the CTLs from vertebrates. The CTLs from insects, molluscs and crustaceans were well separated and clustered together into the other invertebrate group (Fig. 2B).

The distribution of AjSJL-1 mRNA in tissues

*Aj*SJL-1 mRNA transcripts were found to be distributed in all the examined tissues of sea cucumber *A. japonicus*, with the highest level in respiratory tree and the lowest level in coelomocytes. The expression levels were significantly higher in respiratory tree (27.26-fold, $p < 0.01$), body wall (10.38-fold, $p < 0.01$) and tube-foot (4.70-fold, $p < 0.05$) than that in coelomocytes (Fig. 3A).

Temporal expression of AjSJL-1 in coelomocytes after the V. splendidus stimulation

The mRNA expression level of *Aj*SJL-1 in coelomocytes was monitored post the stimulation with *V. splendidus*. It was significantly up-regulated at 6 h (5.01-fold of that in control group, $p < 0.05$), reached the highest level at 12 h (19.27-fold of that in control group, $p < 0.01$), down-regulated sharply at 24 h, and increased again at 48 h (9.22-fold of that in control group, $p < 0.01$) after stimulation (Fig. 3B).

The recombination protein of AjSJL-1 and the specificity of its polyclonal antibody.

The recombinant plasmid (pET-22b-*Aj*SJL-1) was transformed into Transetta (DE3). After IPTG induction with shake (100 rpm) at 16 °C for 12 h, the whole cell lysate was analyzed by 12 % SDS–PAGE. A distinct band was revealed with a molecular mass of 26 kDa, which was consistent with the predicted molecular mass of *Aj*SJL-1 plus His-Tag (Fig. 4A).

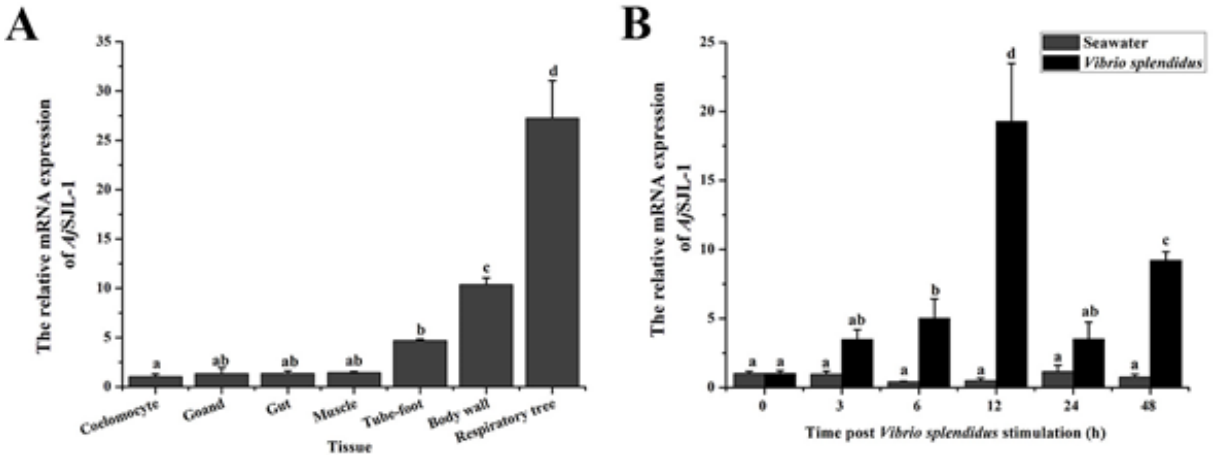

Fig. 3 The temporal and spatial expression patterns of *Aj*SJL-1 mRNA. A: *Aj*SJL-1 mRNA expression in different tissues of sea cucumber *A. japonicus*. Vertical bars represent the mean ± S.D (N =3). The different letters indicate significant differences comparing with other groups ($p < 0.05$, ANOVA). B: The mRNA expression levels of *Aj*SJL-1 in coelomocyte of *A. japonicus* after *V. splendidus* challenge. The *cytb* gene was used as an internal control to calibrate the cDNA template for all the samples. Each value is shown as mean ± S.D. (N =3). The different letters indicate significant differences comparing with other groups ($p < 0.05$, ANOVA)

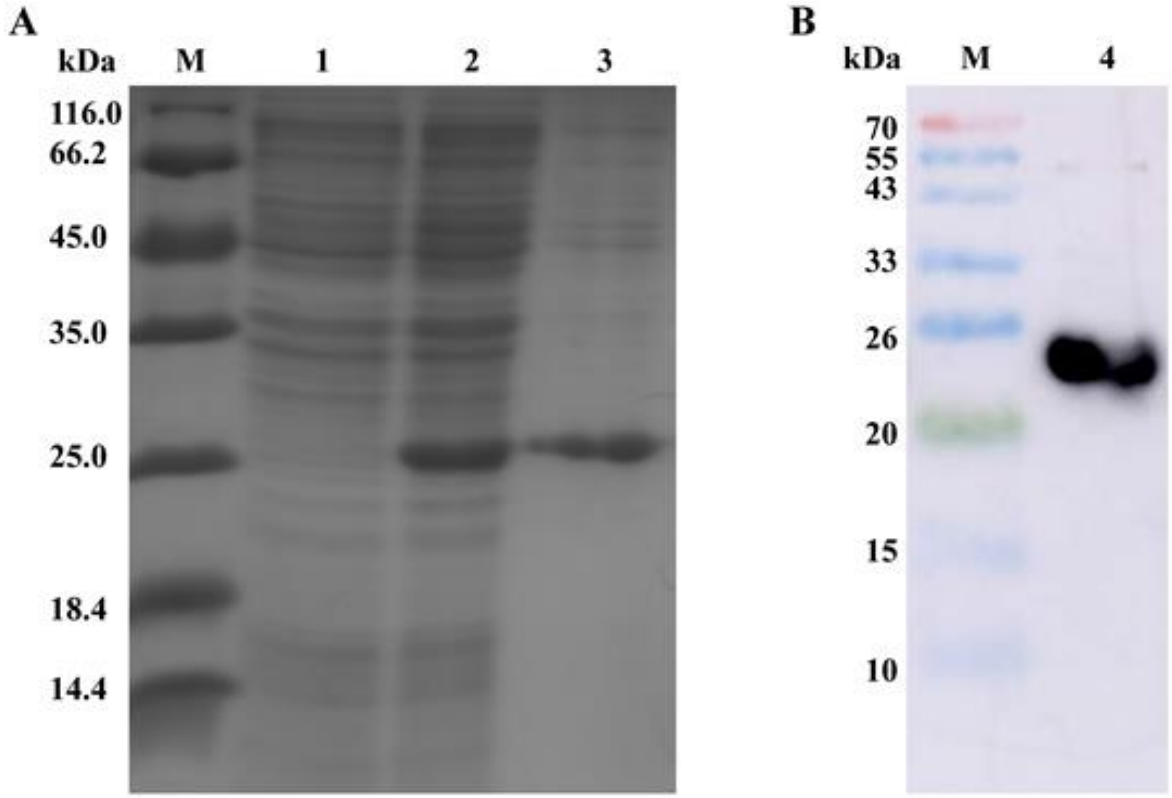

Fig. 4 The recombinant protein of *Aj*SJL-1 and the specificity for its polyclonal antibodies. A: SDS-PAGE analyzes of r*Aj*SJL-1. Lane M: standard protein molecular weight marker; Lane 1: blank control for r*Aj*SJL-1 (without plasmid pET-22b-*Aj*SJL-1); Lane 2: IPTG-induced expression of r*Aj*SJL-1; Lane 3: purified r*Aj*SJL-1. B: Western blot analyzes of the specificity of polyclonal antibody. Lane M: standard protein molecular weight marker; Lane 4: western-bolt based on the sample of purified r*Aj*SJL-1

The purified r*Aj*SJL-1 was used to prepare antibody, and the specificity of the antibody against r*Aj*SJL-1 was assayed by western blotting. A clear reaction band with 26 kDa was revealed (Fig. 4B). No visible reaction band was found in the negative control (data not shown).

Carbohydrate binding capacity of AjSJL-1

The binding assay was performed to examine the PAMPs binding spectrum of *Aj*SJL-1. The PAMP binding capacity was recorded as P/N at 405 nm, and the samples with P/N > 2.1 were considered as positive. In the presence of Ca^{2+}, P/N values of r*Aj*SJL-1 toward LPS, PGN, D-galactose and Man were all higher than 2.1 (Fig. 5A). r*Aj*SJL-1 exhibited relatively higher affinity to PGN and Man, with the minimum concentration of 0.005 mg/mL. Its affinity to D-galactose and LPS was lower with the minimum concentration of 0.025 mg/mL. The values of P/N increased correspondingly with the increasing of r*Aj*SJL-1 concentration, which suggested that the binding activities of r*Aj*SJL-1 towards PGN, Man, D-galactose and LPS were of dose-dependence. In the absence of Ca^{2+}, the P/N values of r*Aj*SJL-1 toward four PAMPs were all less than 2.1 (Fig. 5B). As control, the P/N values of rTrx for all the examined PAMPs were less than 2.1 (data not shown).

Microbial binding activity of rAjSJL-1

The microbe binding assay was carried out to determine the ability of r*Aj*SJL-1 to bind Gram-negative bacteria, Gram-positive bacteria and fungi. In the presence of Ca^{2+}, a strong band was detected for *V. splendidus,* and shallow bands were detected for *S. aureus*, *B. breve*, *P. pastoris* and *Y. lipolytica.* However, when microbes were incubated with r*Aj*SJL-1 in the absence of Ca^{2+}, there were no visible bands detected in all the lanes (Fig. 6A). The result suggested that r*Aj*SJL-1 displayed no obviously binding ability towards the tested microbes without Ca^{2+}. As a control, no binding affinity was found in the group of rTrx-His (Fig. 6B).

Discussion

CTL is a key type of PRR to play significant roles in pathogen recognition through binding to the terminal sugars of glycoprotein in a Ca^{2+} dependent manner. In the past decades, an increasing number of CTLs have been identified in various species (Mcnulty *et al.*, 2012; Zhang *et al.*, 2012; Huang *et al.*, 2014; Zhang *et al.*, 2017), which function in immune response either as cytomembrane receptors in immunocytes or as soluble proteins existing in tissue fluids (Wang *et al.*, 2012; Huang *et al.*, 2013a; Hoving *et al.*, 2014).

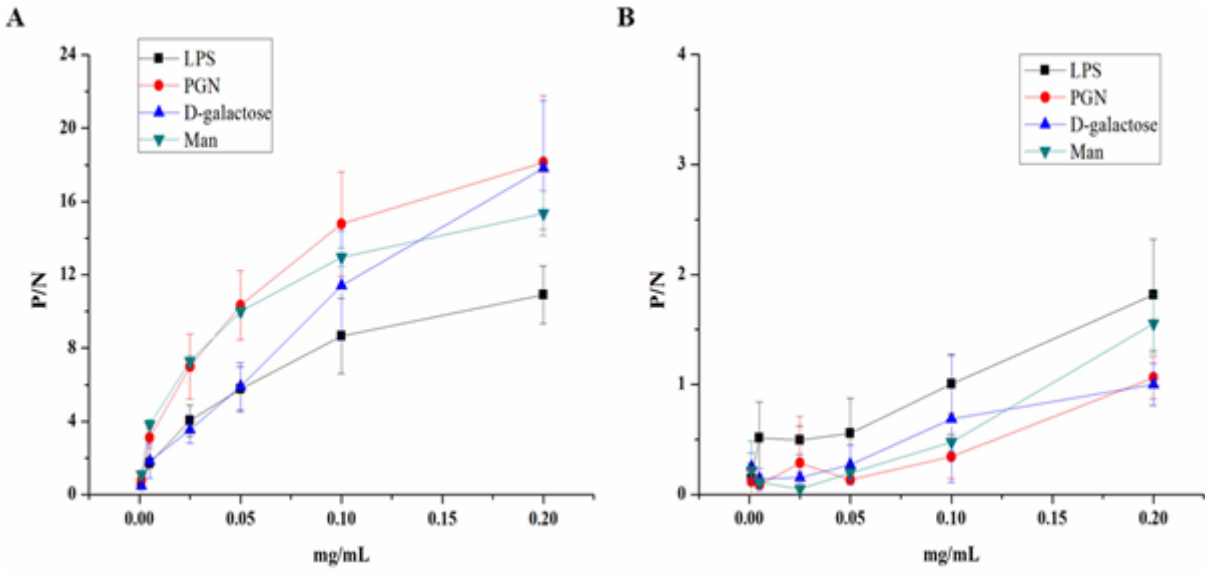

Fig. 5 The interaction between r*Aj*SJL-1 and the PAMPs revealed by ELISA analysis. A: The interaction between r*Aj*SJL-1 and the PAMPs with TBS-Ca^{2+} buffer. B: The interaction between r*Aj*SJL-1 and the PAMPs with TBS buffer. Each value is shown as mean ± S.D. (N =3)

The CTLs harbor at least one CRD, and every CRD has four Ca^{2+}-binding sites, in which Ca^{2+}-binding site 2 is considered as the key site to determine the binding spectrum of CTL (Drickamer, 1999; Zelensky and Gready, 2005; Wang *et al.*, 2011). In Ca^{2+}-binding site 2, there are two conserved motifs determining the CRD binding ability, and the first one is always EPN or QPD in vertebrates (Weis *et al.*, 1998; Zelensky and Gready, 2005). It is found that the motifs in the invertebrate CTLs are more diversified than the vertebrate ones. *Aj*SJL-1 was previously identified as a CTL in sea cucumber containing only one CRD with 163 amino acid residues (Ono *et al*., 2018). Six conserved cysteine residues (Cys^{35}, Cys^{52}, Cys^{118}, Cys^{138}, Cys^{157} and Cys^{161}) were found in the Ca^{2+} binding site 2 of *Aj*SJL-1, among which Cys^{157} and Cys^{161} allowed the CRD to adopt a typical long-form double-loop structure (Drickamer, 1999). In the present study, a novel DPN/WVD motif was identified in the Ca^{2+} binding site 2 of CRD from *Aj*SJL-1, which was different from the previously reported motifs of *AJ*CTL (EPN/WTD) (Han *et al.*, 2012), *Aj*CTL-1 (EPN/WND) and *Aj*CTL-2 (EPN/WND). In the phylogenetic tree, *Aj*SJL-1 was closer to CTL-19s from vertebrate. These results indicated that there was functional differentiation among *Aj*SJL-1 and other CTLs from *A. japonicus*. DPN was only found in Gal/GalNAc lectin from *Entamoeba histolytica*, which was able to recognize galactose/N-acetylgalac-tosamine (Weber *et al.*, 2006; Yadav *et al.*, 2016). It is implied that *Aj*SJL-1 might display similar recognition ability to Gal/GalNAc lectin from *E. histolytica*. All these results indicated that *Aj*SJL-1 was a member of the CTL with novel DPN/WVD motifs in sea cucumber *A. japonicus*.

The distribution of *Aj*SJL-1 mRNA and the alternation of its expression level in coelomocyte after bacterial challenge were examined to understand its involvement in the immune response of sea cucumber. *Aj*SJL-1 mRNA transcripts were found to be widely expressed in water pipe system of sea cucumber, with the highest expression level in respiratory trees (Ono *et al.*, 2018). *Aj*CTL-1 was reported to be highly expressed in gonad and functioned as a PRR in *A. japonicus* to recognize microbes (Wei *et al.*, 2015). *Aj*CTL-2 was highly expressed in coelomocyte, indicating that it might be an important molecule in the coelomocyte mediated immune defense (Wang *et al.*, 2018). The different expression profiles of those CTLs in tissues indicated that they might execute different functions in the innate immunity of *A. japonicus*. Respiratory tree is considered as a unique tissue for breathing in *A. japonica*. The higher expressions of *Aj*SJL-1 in respiratory tree suggested that *Aj*SJL-1 might play an important role in mucosal immunity of sea cucumber. Coelomocytes are the main component of the immune system and play important roles in sea cucumber to resist pathogen invasion (Wang *et al.*, 2015). When the sea cucumbers were challenged by *V. splendidus*, the expression level of *Aj*SJL-1 mRNA in coelomocyte increased significantly ($p < 0.01$) at 12 h, suggesting it was induced by immune stimulation similar to the CTLs in other invertebrates (Wang *et al.*, 2012; Drummond and Brown, 2013; Huang *et al.*, 2013a; Huang *et al.*, 2013b; Li *et al.*, 2015a; Yang *et al.*, 2015; Zhou and Sun, 2015). All these results indicated that *Aj*SJL-1 was involved in the immune response against microbial infection.

The protein-carbohydrate interaction mediated by CTLs is benefited from their CRDs, and the conserved motifs at the Ca^{2+}-binding site 2 of CRDs determine their binding ability (Kong *et al.*, 2011; Huang *et al.*, 2013b; Yang *et al.*, 2015). In the present

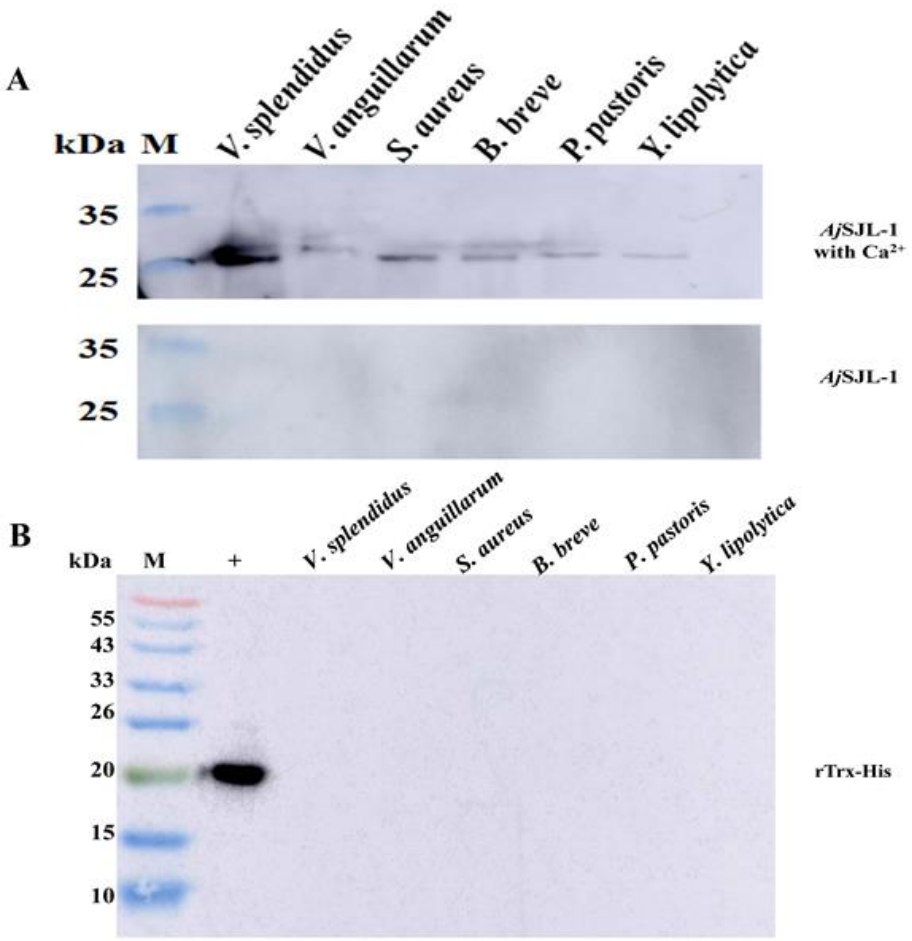

Fig. 6 The microbe binding activity of r*Aj*SJL-1 and rTrx revealed by western blotting. A: The microbe binding activity of r*Aj*SJL-1 with TBS-Ca^{2+} or TBS buffer. B: The microbe binding activity of rTrx. Lane M: pre-stained marker (kDa); Lane 1: *V. splendidus*; Lane 2: *V. anguillarum*; Lane 3: *S. aureus*; Lane 4: *B. breve*; Lane 5: *P. pastoris*; Lane 6: *Y. lipolytica*

study, *Aj*SJL-1 was found to bind all the tested PAMPs including LPS, PGN, mannose and D-galactose in a Ca^{2+} dependent manner. It is noteworthy that a new DPN/WVD motif was found in the CRD of *Aj*SJL-1. Different from the previously identified Gal/GalNAc lectin from *E. histolytica* with DPN motif to recognize galactose/N-acetylgalactosamine (Weber *et al.*, 2006; Yadav *et al.*, 2016), the new DPN/WVD motif gifted *Aj*SJL-1 with the broad-spectrum binding activity. It is a common feature for all the identified vertebrate and invertebrate CRDs that the second amino acid in the motifs of Ca^{2+} binding site 2 is always "Pro" (Mitra and Das, 2001; Wei *et al.*, 2012; De Melo *et al.*, 2014; Drickamer and Taylor, 2015; Zhou and Sun, 2015). Structurally, the side chain of "Pro" is essential to keep the stability and bind metal ion (Zelensky and Gready, 2005; Yang *et al.*, 2015). Moreover, the first and third amino acid in the motifs of Ca^{2+}-binding site 2 affects the binding spectrum of CRD (Mullin *et al.*, 1997; Zelensky and Gready, 2005; Wang *et al.*, 2012). In the present study, the DPN motif endowed *Aj*SJL-1 with binding activity to various PAMPs, which was different from the specific binding capability of EPN and QPD in vertebrate CTL. According to previous report that the third amino acid "Asn" in the motif of Ca^{2+}-binding site 2 determined the binding specificity of CTL towards mannose (Yang *et al.*, 2015), the first amino acid "Asp" in the motif of *Aj*SJL-1 might be the key determinant for its binding activity to D-galactose (Yadav *et al.*, 2016). In addition, compared with *Aj*CTL-2, *Aj*SJL-1 displayed stronger binding ability to various PAMPs, which was suspected to be determined by the WVD motif. The second motif has been reported to affect the affinity with carbohydrates (Zelensky and Gready, 2005; Yang *et al.*, 2015). *Aj*SJL-1 lost its binding ability to all PAMPs in the absence of Ca^{2+}. These results collectively suggested that *Aj*SJL-1 was a Ca^{2+}-dependent CTL with novel DPN/WVD motifs responsible for the recognition of diverse PAMPs in immune response of sea cucumber.

The predominant microbe recognition and binding capability of CTLs make them indispensable in the first defense line against pathogen infection (Drummond and Brown, 2013). In the present study,

*Aj*SJL-1 was found to bind Gram-negative bacteria, Gram-positive bacteria and fungi in the presence of Ca^{2+}, which was consistent with its broad binding spectrum to PAMPs. The broad microbe binding spectrum manifested its indispensable roles in innate immunity (Yu *et al.*, 2007), which favored that *Aj*SJL-1 was involved in immune response against various pathogens as a PRR. It was previously found that some CTLs with a single CRD identified from invertebrates could bind to limited spectrum of microorganisms. For instance, *Ai*CTL-7 only aggregated *P. pastoris* (Kong *et al.*, 2011), and *Cg*CLec-2 was able to bind LPS, PGN, mannan and zymosan rather than β-glucan (Yang *et al.*, 2010). Considering that there was a novel DPN/WVD motif in the Ca^{2+}-binding site 2 of *Aj*SJL-1, it was speculated that this new DPN/WVD motifs might endow *Aj*SJL-1 with a broad recognition spectrum of microorganisms.

In conclusion, *Aj*SJL-1 was characterized as a new member of CTL family with novel DPN/WVD motifs in sea cucumber *A. japonicus*. *Aj*SJL-1 mRNA was highly expressed in the respiratory tree, and its expression level in coelomocyte increased significantly at 12 h after *V. splendidus* stimulation. It recognized and bound various PAMPs and microbes with broad spectrum.

Acknowledgement

We are grateful to all the laboratory members for their technical advice and helpful discussions. This research was supported by National Key R&D Program (2018YFD0900606), the National Natural Science Foundation of China (No. 31530059), the Distinguished Professor of Liaoning (XLYC19020120), the Scientific Research Project of Liaoning Province Department of Education (No. L2014284), AoShan Talents Cultivation Program Supported by Qingdao National Laboratory for Marine Science and Technology (No. 2017ASTCP-OS13), the Research Foundation for Talented Scholars in Dalian Ocean University (to L. S.), and the Startup Foundation for Doctoral of Dalian ocean university (No. HDYJ201407).

References

Arnold K, Bordoli L, Kopp J, Schwede T. The SWISS-MODEL workspace: a web-based environment for protein structure homology modelling. Bioinformatics 22: 195-201, 2006.

De Melo AA, Carneiro RF, Silva WDM, Moura RDM, Silva GC, De Sousa OV, et al. HGA-2, a novel galactoside-binding lectin from the sea cucumber Holothuria grisea binds to bacterial cells. Int. J. Biol. Macromol. 64: 435-442, 2014.

Devi RV, Basilrose MR, Mercy PD. Prospect for lectins in arthropods. Ital. J. Zool. 77: 254-260, 2010.

Drickamer K. Engineering galactose-binding activity into a C-type mannose-binding protein. Nature 360: 183-186, 1992.

Drickamer K. C-type lectin-like domains. Curr. Opin. Struct. Biol. 9: 585-590, 1999.

Drickamer K, Taylor ME. Biology of Animal Lectins. Annu. Rev. Cell Biol. 9: 237-264, 1993.

Drickamer K, Taylor ME. Recent insights into structures and functions of C-type lectins in the immune system. Curr. Opin. Struct. Biol. 34: 26-34, 2015.

Drummond RA, Brown GD. Signalling C-type lectins in antimicrobial immunity. PLoS Pathog. 9: e1003417, 2013.

East L, Isacke C. The mannose receptor family. Biochim. Biophys. Acta, Gen. Subj. 1572: 364-386, 2002.

Han LL, Yuan Z, Dahms HU, Li QY, Zhang QZ, Wu RJ, et al. Molecular cloning, characterization and expression analysis of a C-type lectin (*AJ*CTL) from the sea cucumber *Apostichopus japonicus*. Immunol. Lett. 143: 137-145, 2012.

Hoving JC, Wilson GJ, Brown GD. Signalling C-type lectin receptors, microbial recognition and immunity. Cell. Microbiol. 16: 185-194, 2014.

Huang M, Song X, Zhao J, Mu C, Wang L, Zhang H, *et al*. A C-type lectin (*Ai*CTL-3) from bay scallop *Argopecten irradians* with mannose/galactose binding ability to bind various bacteria. Gene 531: 31-38, 2013a.

Huang M, Wang L, Yang J, Zhang H, Wang L, Song L. A four-CRD C-type lectin from *Chlamys farreri* mediating nonself-recognition with broader spectrum and opsonization. Dev. Comp. Immunol. 39: 363-369, 2013b.

Huang M, Zhang H, Jiang S, Wang L, Liu R, Yi Q, *et al*. An EPD/WSD motifs containing C-type lectin from *Argopectens irradians* recognizes and binds microbes with broad spectrum. Fish Shellfish Immunol. 43: 287-293, 2015.

Huang S, Chen Z, Yan X, Yu T, Huang G, Yan Q, *et al*. Decelerated genome evolution in modern vertebrates revealed by analysis of multiple lancelet genomes. Nat. Commun. 5: 5896-5896, 2014.

Jiang J, Zhou Z, Dong Y, Cong C, Guan X, Wang B, *et al*. *In vitro* antibacterial analysis of phenoloxidase reaction products from the sea cucumber *Apostichopus japonicus*. Fish Shellfish Immunol. 39: 458-463, 2014.

Kiefer F, Arnold K, Kunzli M, Bordoli L, Schwede T. The SWISS-MODEL Repository and associated resources. Nucleic Acids Res. 37: 387-392, 2009.

Kong P, Wang L, Zhang H, Song X, Zhou Z, Yang J, *et al*. A novel C-type lectin from bay scallop *Argopecten irradians* (*Ai*CTL-7) agglutinating fungi with mannose specificity. Fish Shellfish Immunol. 30: 836-844, 2011.

Kumar S, Tamura K, Nei M. MEGA3: Integrated software for Molecular Evolutionary Genetics Analysis and sequence alignment. Briefings Bioinf. 5: 150-163, 2004.

Li H, Chen Y, Li M, Wang S, Zuo H, Xu X, *et al*. A C-type lectin (*Lv*CTL4) from *Litopenaeus vannamei* is a downstream molecule of the NF-κB signaling pathway and participates in antibacterial immune response. Fish Shellfish Immunol. 43: 257-263, 2015a.

Li H, Zhang H, Jiang S, Wang W, Xin L, Wang H, *et al*. A single-CRD C-type lectin from oyster *Crassostrea gigas* mediates immune recognition and pathogen elimination with a potential role in the activation of complement system. Fish Shellfish Immunol. 44: 566-575, 2015b.

Liu Y, Wang W, Zhao Q, Yuan P, Li J, Song X, *et al*. A DM9-containing protein from oyster *Crassostrea gigas* (*Cg*DM9CP-3) mediating immune recognition and encapsulation. Dev. Comp. Immunol. 116: 103937, 2021.

Livak KJ, Schmittgen TD. Analysis of relative gene expression data using real-time quantitative PCR and the 2(-Delta Delta C(T)) Method. Methods 25: 402-408, 2001.

Loizou S, McCrea J, Rudge A, Reynolds R, Boyle C, Harris E. Measurement of anti-cardiolipin antibodies by an enzyme-linked immunosorbent assay (ELISA): standardization and quantitation of results. Clin. Exp. Immunol. 62: 738, 1985.

Mcnulty SN, Mullin AS, Vaughan JA, Tkach VV, Weil GJ, Fischer PU. Comparing the mitochondrial genomes of Wolbachia -dependent and independent filarial nematode species. BMC Genomics 13: 145-145, 2012.

Mitra S, Das HR. A novel mannose-binding lectin from plasma of Labeo rohita. Fish Physiol. Biochem. 25: 121-129, 2001.

Mullin NP, Hitchen PG, Taylor ME. Mechanism of Ca^{2+} and Monosaccharide Binding to a C-type Carbohydrate-recognition Domain of the Macrophage Mannose Receptor. J. Biol. Chem. 272: 5668-5681, 1997.

Ono K, Suzuki TA, Toyoshima Y, Suzuki T, Tsutsui S, Odaka T, *et al*. SJL-1, a C-type lectin, acts as a surface defense molecule in Japanese sea cucumber, *Apostichopus japonicus*. Mol. Immunol. 97: 63-70, 2018.

Ren C, Chen T, Jiang X, Wang Y, Hu C. Identification and functional characterization of a novel ferritin subunit from the tropical sea cucumber, *Stichopus monotuberculatus*. Fish Shellfish Immunol. 38: 265-274, 2014.

Su Y, Liu Y, Gao F, Cui Z. A novel C-type lectin with a YPD motif from *Portunus trituberculatus* (*Pt*CLec1) mediating pathogen recognition and opsonization. Dev. Comp. Immunol. 106: 103609, 2020.

Sun X, Li Q, Kong L. Comparative mitochondrial genomics within sea cucumber (*Apostichopus japonicus*): Provide new insights into relationships among color variants. Aquaculture 309: 280-285, 2010.

Wang H, Song L, Li C, Zhao J, Zhang H, Ni D, *et al*. Cloning and characterization of a novel C-type lectin from Zhikong scallop *Chlamys farreri*. Mol. Immunol. 44: 722-731, 2007.

Wang H, Xue Z, Liu Z, Wang W, Wang F, Wang Y, *et al*. A novel C-type lectin from the sea cucumber *Apostichopus japonicus* (*Aj*CTL-2) with preferential binding of d-galactose. Fish Shellfish Immunol. 79: 218-227, 2018.

Wang L, Huang M, Zhang H, Song L. The immune role of C-type lectins in molluscs. ISJ-Invertebrate Survival Journal 8: 241-246, 2011.

Wang L, Wang L, Yang J, Zhang H, Huang M, Kong P, *et al*. A multi-CRD C-type lectin with broad recognition spectrum and cellular adhesion from *Argopecten irradians*. Dev. Comp. Immunol. 36: 591-601, 2012.

Wang S, Li T, Xu L, Li L, Fan Y, Wei J. Immunopotentiating Effect of Small Peptides on Primary Culture Coelomocytes of Sea Cucumber, *Apostichopus japonicus*. J. World Aquacult. Soc. 46: 337-343, 2015.

Wang X, Xu W, Zhang X, Zhao X, Yu X, Wang J. A C-type lectin is involved in the innate immune response of Chinese white shrimp. Fish Shellfish Immunol. 27: 556-562, 2009.

Weber C, Guigon G, Bouchier C, Frangeul L, Moreira S, Sismeiro O, *et al*. Stress by Heat Shock Induces Massive Down Regulation of Genes and Allows Differential Allelic Expression of the Gal/GalNAc Lectin in Entamoeba histolytica. Eukaryotic Cell 5: 871-875, 2006.

Wei X, Liu X, Yang J, Fang J, Qiao H, Zhang Y, *et al*. Two C-type lectins from shrimp *Litopenaeus vannamei* that might be involved in immune response against bacteria and virus. Fish Shellfish Immunol. 32: 132-140, 2012.

Wei X, Liu X, Yang J, Wang S, Sun G, Yang J. Critical roles of sea cucumber C-type lectin in non-self recognition and bacterial clearance. Fish Shellfish Immunol. 45: 791-799, 2015.

Weis WI, Taylor ME, Drickamer K. The C-type lectin superfamily in the immune system. Immunol. Rev. 163: 19-34, 1998.

Yadav R, Verma K, Chandra M, Mukherjee M, Datta S. Biophysical studies on calcium and carbohydrate binding to carbohydrate recognition domain of Gal/GalNAc lectin from *Entamoeba histolytica* : insights into host cell adhesion. J. Biochem. 160: 177-186, 2016.

Yan A, Ren C, Chen T, Jiang X, Sun H, Huo D, *et al*. The first tropical sea cucumber caspase-8 from *Holothuria leucospilota*: Molecular characterization, involvement of apoptosis and inducible expression by immune challenge. Fish Shellfish Immunol. 72: 124-131, 2018.

Yang J, Huang M, Zhang H, Wang L, Wang H, Wang L, *et al*. CfLec-3 from scallop: an entrance to non-self recognition mechanism of invertebrate C-type lectin. Sci. Rep. 5: 10068-10068, 2015.

Yang J, Qiu L, Wei X, Wang L, Wang L, Zhou Z, *et al*. An ancient C-type lectin in *Chlamys farreri* (CfLec-2) that mediate pathogen recognition and cellular adhesion. Dev. Comp. Immunol. 34: 1274-1282, 2010.

Yang MC, Shi XZ, Yang HT, Sun JJ, Xu L, Wang XW, *et al*. Scavenger receptor C mediates phagocytosis of white spot syndrome virus and restricts virus proliferation in shrimp. PLoS Pathog. 12: e1006127, 2016.

Yu Y, Yu Y, Huang H, Feng K, Pan M, Yuan S, *et al*. A Short-Form C-Type Lectin from Amphioxus Acts as a Direct Microbial Killing Protein via Interaction with Peptidoglycan and Glucan. J. Immunol. 179: 8425-8434, 2007.

Zelensky AN, Gready JE. The C-type lectin-like domain superfamily. FEBS J. 272: 6179-6217, 2005.

Zhang G, Fang X, Guo X, Li L, Luo R, Xu F, *et al*. The oyster genome reveals stress adaptation and complexity of shell formation. Nature 490: 49-54, 2012.

Zhang H, Wang H, Wang L, Song X, Zhao J, Qiu L, *et al*. A novel C-type lectin (*Cf*lec-3) from *Chlamys farreri* with three carbohydrate-recognition domains. Fish Shellfish Immunol. 26: 707-715, 2009.

Zhang X, Sun L, Yuan J, Sun Y, Gao Y, Zhang L, *et al*. The sea cucumber genome provides insights into morphological evolution and visceral regeneration. PLoS Biol. 15: e2003790, 2017.

Zhou Z, Sun L. CsCTL1, a teleost C-type lectin that promotes antibacterial and antiviral immune defense in a manner that depends on the conserved EPN motif. Dev. Comp. Immunol. 50: 69-77, 2015.